

Scaling violation in power corrections to energy correlators from the light-ray OPE

Hao Chen,¹ Pier Francesco Monni,² Zhen Xu,¹ and Hua Xing Zhu^{3,4}

¹*Zhejiang Institute of Modern Physics, School of Physics, Zhejiang University, Hangzhou, Zhejiang, 310027, China*

²*CERN, Theoretical Physics Department, CH-1211 Geneva 23, Switzerland*

³*School of Physics, Peking University, Beijing, 100871, China*

⁴*Center for High Energy Physics, Peking University, Beijing 100871, China*

In recent years, energy correlators have emerged as a powerful tool to explore the field theoretic structure of strong interactions at particle colliders. In this Letter we initiate a novel study of the non-perturbative power corrections to the projected N -point energy correlators in the limit where the angle between the detectors is small. Using the light-ray operator product expansion (OPE) as a guiding principle, we derive the power corrections in terms of two non-perturbative quantities describing the fragmentation of quarks and gluons. In analogy with their perturbative leading-power counterpart, we show that power corrections obey a classical scaling behavior that is violated at the quantum level. This crucially results in a dependence on the hard scale Q of the problem that is calculable in perturbation theory. Our analytic predictions are successfully tested against Monte Carlo simulations for both lepton and hadron colliders, marking a significant step forward in the understanding of these observables.

Introduction.— Within the physics programme of the Large Hadron Collider (LHC), energy correlators [1–3] have emerged as a powerful tool to study the properties of strong interactions, such as the precise extractions of the strong coupling constant [4]. From a theoretical viewpoint, these observables have inspired a thorough investigation of their field-theoretic properties [5–27]. Owing to their simplicity, energy correlators inherit the quantum properties of the correlation functions, which encode fundamental information about the underlying field theory [28]. This paves the way to new explorations of Quantum Chromodynamics using present and future collider data, as reflected in the wide phenomenological interest they have attracted in particle physics [21, 29–49], heavy-ion physics [50–56] and nuclear physics [57–62].

An N -point energy correlator is defined by weighing the cross section with the product of the energies of N particles (e.g. within a jet), as a function of their relative angles. One can define the corresponding projected N -point energy correlator (ENC) by integrating the resulting correlator over these angles except for the largest one θ_L , as a univariate function of the angular variable $x_L \equiv (1 - \cos \theta_L)/2$ [3]. In the collinear limit, considered in this Letter, one is interested in the regime in which such angular variable is parametrically small, i.e. $\sqrt{x_L}Q \ll Q$, with Q being the hard momentum transfer of the scattering process. At leading power, the ENC shows a classical scaling behavior $\mathcal{O}(1/x_L)$ in the collinear limit [5–7, 9–13, 29], that is determined by Lorentz symmetry. This scaling is then violated by quantum effects, which induce a mild additional dependence on the hard scale Q . The evolution of ENC with Q can be obtained using perturbative collinear resummation techniques [3, 21, 29, 49, 63–65].

The full exploitation of high-precision experimental data also demands an understanding of the dynamics of ENC beyond perturbation theory. A first-principle understanding of the deep non-perturbative limit in which the angular distance $\sqrt{x_L}$ becomes of the order of the ra-

tio Λ_{QCD}/Q , with Λ_{QCD} being a typical hadronic scale, is currently out of reach. Nevertheless, in the regime $1 \gg \sqrt{x_L} \gg \Lambda_{\text{QCD}}/Q$, one can approximate non-perturbative corrections in a power expansion in Λ_{QCD}/Q , gaining a better analytic control over their properties. The next-to-leading power term of this expansion, commonly denoted as *power correction*, defines the leading non-perturbative correction in this kinematic regime. These power corrections can be studied using a range of analytic techniques, which have been used to investigate observables belonging to the ENC family at lepton colliders both in the bulk of the phase space [66–68] ($x_L \neq 0, 1$) as well as in the back-to-back limit [69] ($x_L \rightarrow 1$).

This Letter initiates a novel study of the ENC in the collinear ($x_L \rightarrow 0$) limit. We will show that, similarly to their leading-power counterpart, the coefficient of the linear $\mathcal{O}(\Lambda_{\text{QCD}}/Q)$ power correction to the ENC exhibits a classical scaling behavior fixed by symmetry arguments, that is violated at the quantum level in a way that can be predicted using perturbation theory. This phenomenon shares similarities with the violation of the well known Bjorken scaling [70–73], where the evolution of the non-perturbative structure functions with the scale is fully perturbative [71–73]. Using the light-ray OPE [5, 7, 9–11, 74], we are able to calculate the evolution of the power correction with the energy scale Q , hence predicting how they are related at different scales. This result marks a significant step forward in the theoretical understanding of this class of observables beyond the perturbative level.

ENC and the light-ray OPE.— The projected energy correlators (ENC) are correlation functions of the energy flow operators $\mathcal{E}(n)$ in a physical state $|\Psi_q\rangle$ [1, 2, 5], defined as $\langle \mathcal{E}(n_1) \cdots \mathcal{E}(n_k) \rangle_{\Psi_q} \equiv \langle \Psi_q | \mathcal{E}(n_1) \cdots \mathcal{E}(n_k) | \Psi_q \rangle$, where q^μ is the total momentum of the state $|\Psi_q\rangle$. The energy flow operator $\mathcal{E}(n)$ is defined as [5, 75]

$$\mathcal{E}(n) = \mathbb{L}_{\tau=2} [n^i T_{0i}(t, r\vec{n})] , \quad (1)$$

where $T_{\mu\nu}$ is the energy-momentum tensor of QCD and the operation \mathbb{L}_τ is the light transform [76]

$$\mathbb{L}_\tau = \lim_{r \rightarrow \infty} r^\tau \int_0^\infty dt. \quad (2)$$

Examples for the state $|\Psi_q\rangle$ include those excited by the electromagnetic current from the vacuum, the decay products of a Higgs boson, or the scattering state of a high-energy collision. Generic final states consist of the ensemble described by the density $\rho_q = \sum_\Psi |\Psi_q\rangle\langle\Psi_q|$.

In recent years, the light-ray OPE has emerged as an efficient tool to study energy correlators in the small angle limit. Originally developed in the context of conformal collider physics [5, 7, 9], the light-ray OPE has recently been found useful also in QCD [10, 11, 74]. For the simplest two-point energy correlator (EEC), the light-ray OPE at leading twist reads

$$\begin{aligned} \lim_{n_1 \rightarrow n_2} \mathcal{E}(n_1)\mathcal{E}(n_2) &= \frac{1}{x_L} \vec{C} \cdot \vec{\mathcal{O}}_{\tau=2}^{[J=3]}(n_2) \\ &+ \frac{\Lambda_{\text{QCD}}}{x_L^{3/2}} \vec{D} \cdot \vec{\mathcal{O}}_{\tau=2}^{[J=2]}(n_2) + \dots, \end{aligned} \quad (3)$$

where $x_L = (n_1 \cdot n_2)/2$ is related to the angular distance of two light-like directions n_1 and n_2 , and \vec{C} , \vec{D} are dimensionless OPE coefficients. The light-ray OPE formula in (3) describes the leading small-angle behavior of the EEC. The operator $\vec{\mathcal{O}}_{\tau=2}^{[J]}$ belongs to the leading trajectory of the light-ray operator [76]. For *even* collinear spin J , it can be obtained by a light transform of the following twist $\tau = 2$ local operators [10, 11]:

$$\vec{\mathcal{O}}_{\tau=2}^{[J]} = \mathbb{L}_2[\vec{\mathcal{O}}_{\tau=2}^{[J]}], \quad \vec{\mathcal{O}}_{\tau=2}^{[J]} = \begin{pmatrix} \frac{1}{2^J} \bar{\psi} \gamma^+ (iD^+)^{J-1} \psi \\ \frac{-1}{2^J} G^{a,\mu+} (iD^+)^{J-2} G_\mu^{a,+} \end{pmatrix}, \quad (4)$$

where $\gamma^+ = \bar{n} \cdot \gamma$, and $\tau = \Delta - J$, where Δ is the operator dimension. The energy flow operator corresponds to the combination $\mathcal{E} = (1, 1) \cdot \vec{\mathcal{O}}_{\tau=2}^{[J=2]}$, with $J = 2$.

The form of the light-ray OPE (3) is determined by dimensional analysis and Lorentz symmetry. To understand this, we collect in TABLE I the collinear spin and dimension of all the ingredients entering the OPE (3). By dimensional analysis, imposing that the dimension of both sides of (3) is the same fixes the dimension of the operators in each term of the light-ray OPE. Imposing that the light-ray operators have twist label $\tau = 2$ fixes their collinear spin, which determines the label $J = 3$ for the first term in (3) and $J = 2$ for the $\mathcal{O}(\Lambda_{\text{QCD}}/Q)$ power correction. This completely determines the classical scaling in x_L , e.g. $x_L^{-3/2}$ for the $\mathcal{O}(\Lambda_{\text{QCD}}/Q)$ term. The reason is that the collinear spin of x_L is completely fixed by its transformation properties under a Lorentz boost, which acts as a dilation of angles on the celestial sphere, as depicted in FIG. 1. Using the quantities listed in TABLE I, it is easy to verify the legitimacy of (3) (cf. [77] for further discussions).

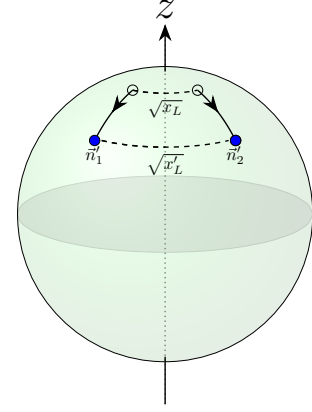


FIG. 1: A boost in the positive z direction increases the distance of two energy flow operator on the celestial sphere.

	\mathbb{L}_τ	$\vec{\mathcal{O}}_\tau^{[J]}$	$\vec{\mathcal{O}}_\tau^{[J]}$	$ x_L $	Λ_{QCD}, Q
coll. spin	$1 - \tau$	$-J$	$1 - (\tau + J)$	2	0
dimension	$-\tau - 1$	$\tau + J$	$J - 1$	0	1

TABLE I: Collinear spin (boost) and classical scaling dimension of various quantities appearing in the OPE (3).

The light-ray OPE in (3) can be generalized to higher point correlators. For N energy flow operators, the observable depends on $N(N-1)/2$ angles for an isotropic state $|\Psi_q\rangle$. We are interested in the projective N -point energy correlator, where the higher dimensional distribution is projected to the axis of the maximal angular distance of the N energy flow operators. In this case the OPE formula reads

$$\begin{aligned} \int d\bar{\Omega} \lim_{n_i \rightarrow n} \mathcal{E}(n_1) \cdots \mathcal{E}(n_N) &= \frac{1}{x_L} \vec{C}_N \cdot \vec{\mathcal{O}}_{\tau=2}^{[J=N+1]}(n) \\ &+ \frac{\Lambda_{\text{QCD}}}{x_L^{3/2}} \vec{D}_N \cdot \vec{\mathcal{O}}_{\tau=2}^{[J=N]}(n) + \dots \end{aligned} \quad (5)$$

where all n_i directions approach n . The angular integral is over the $N(N-1)/2 - 1$ angles except the largest separation x_L among the N directions. The general N -point projective energy correlator can be defined as the normalized expectation value of the product of N energy flow operators in a state $|\Psi_q\rangle$:

$$\text{ENC}_{\Psi_q}(x_L, Q) = \frac{4\pi}{\sigma_{\Psi_q} Q^N} \int d\bar{\Omega} \lim_{n_i \rightarrow n} \langle \mathcal{E}(n_1) \cdots \mathcal{E}(n_N) \rangle_{\Psi_q}, \quad (6)$$

where $\sigma_{\Psi_q} = \langle \Psi_q | \Psi_q \rangle$ and $Q = q^0$ is the energy of the state, e.g. the center-of-mass energy in $\gamma^* \rightarrow q\bar{q}$ or $h \rightarrow gg$, or the energy of jets.

For $N = 2$ it reduces to the conventional EEC [1, 2]. In parton language, the first term in the r.h.s. of Eq. (3)

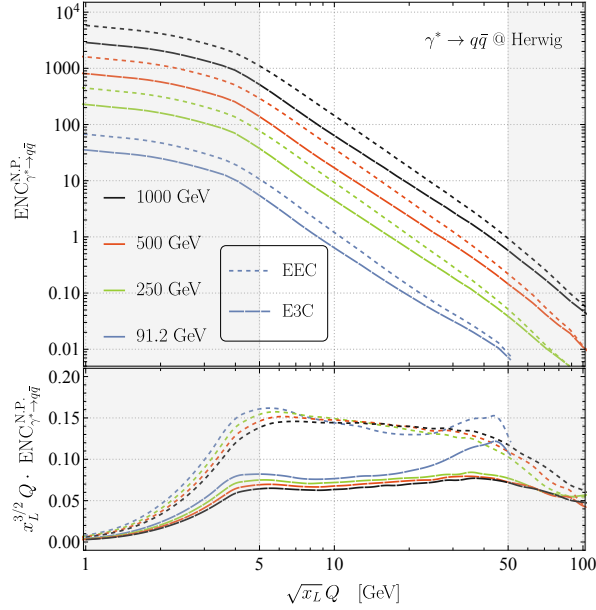


FIG. 2: The upper panel shows the classical scaling of the energy correlators across energy and angular scales. The lower panel highlights the mild quantum scaling violation.

gives rise to the factorisation theorem of Refs. [3, 29], known at Next-to-Next-to-Leading Logarithmic (NNLL) accuracy in QCD [29, 49]. The operators $\tilde{\mathcal{O}}_{\tau=2}^{[J=3]}$ are mapped onto the hard function while the OPE coefficients are encoded in the jet function. The leading-power EEC exhibits a classical scaling behavior $\mathcal{O}(1/x_L)$, which is mildly violated by quantum corrections that modify its dependence on the energy Q . Analogous considerations hold for the ENC starting from Eq. (5).

We now focus on the power correction to the N -point projective energy correlator by defining

$$\text{ENC}_{\Psi_q}^{\text{N.P.}}(x_L, Q) \equiv \text{ENC}_{\Psi_q}(x_L, Q) - \text{ENC}_{\Psi_q}^{\text{P.T.}}(x_L, Q), \quad (7)$$

where the subscript P.T. denotes the leading power, perturbative part of the energy correlator. Eq. (5) predicts a classical scaling behavior $\mathcal{O}(x_L^{-3/2})$ for the leading power correction. The assumption of linearity in Λ_{QCD} is supported by predictions from hadronization [2, 78], Wilson loop [66, 67] and renormalon [68] models.

The classical scaling can be verified using Monte Carlo simulations for e^+e^- collision at different Q , as shown in FIG.2 for the process $\gamma^* \rightarrow q\bar{q}$. In the following we consider the regime $Q \gg Q\sqrt{x_L} \gg \Lambda_{\text{QCD}}$, shown in the unshaded region of the plot, where the scaling is clearly visible.

Scaling violation in power corrections.— The above discussion about classical scaling is based only on Lorentz symmetry and classical dimensional analysis. We now show that the OPE also predicts quantum corrections that slightly violate this scaling in the perturbative region

$Q \gg Q\sqrt{x_L} \gg \Lambda_{\text{QCD}}$. We start by factoring out the classical scaling of $\text{ENC}_{\Psi_q}^{\text{N.P.}}(x_L, Q)$, and write

$$\text{ENC}_{\Psi_q}^{\text{N.P.}}(x_L, Q) = \frac{\text{ENC}_{1, \Psi_q}^{\text{N.P.}}(K_\perp, Q)}{x_L^{3/2} Q} + \dots, \quad (8)$$

where $K_\perp = \sqrt{x_L} Q$ characterizes the exchanged transverse momentum scale and we neglected subleading power corrections in the r.h.s. Classically, no dependence of $\text{ENC}_{1, \Psi_q}^{\text{N.P.}}(K_\perp, Q)$ on Q is expected. At the quantum level, the function $\text{ENC}_{1, \Psi_q}^{\text{N.P.}}(K_\perp, Q)$ mildly depends on Q . This can be appreciated in the lower panel of FIG. 2, where the classical scaling has been removed. We refer to the small residual dependence of $\text{ENC}_{1, \Psi_q}^{\text{N.P.}}(K_\perp, Q)$ on Q as to quantum *scaling violation*.

We now show how the scaling violation is caused by the renormalization group (RG) evolution of $\tilde{\mathcal{O}}_{\tau=2}^{[J]}$. The light-ray OPE (5) provides the following factorized prediction for $\text{ENC}_{1, \Psi_q}^{\text{N.P.}}$

$$\begin{aligned} \text{ENC}_{1, \Psi_q}^{\text{N.P.}}(K_\perp, Q) &= \Lambda_{\text{QCD}} \\ &\times \bar{D}_N \left(\frac{K_\perp^2}{\mu^2}, \frac{\Lambda_{\text{QCD}}^2}{\mu^2} \right) \cdot \frac{\langle \tilde{\mathcal{O}}_{\tau=2}^{[J=N]}(n; \mu) \rangle_{\Psi_q}}{(4\pi)^{-1} \sigma_{\Psi_q} Q^{N-1}} \left(\frac{Q^2}{\mu^2} \right), \end{aligned} \quad (9)$$

where μ is a factorization scale that separates the perturbative matrix element of light-ray operators and the non-perturbative OPE coefficients \bar{D}_N , which also depend on Λ_{QCD} . The light-ray operator $\tilde{\mathcal{O}}_{\tau=2}^{[J]}(n; \mu)$ satisfies the DGLAP equation [10, 11, 74, 79]

$$\mu \frac{d}{d\mu} \tilde{\mathcal{O}}_{\tau=2}^{[J]}(n; \mu) = \gamma_{\tau=2}^{[J]}(\mu) \cdot \tilde{\mathcal{O}}_{\tau=2}^{[J]}(n; \mu), \quad (10)$$

where $\gamma_{\tau=2}^{[J=N]}$ is the anomalous dimension matrix of the twist-2 light-ray operators, which admits the perturbative expansion $\gamma_{\tau=2}^{[J]}(\mu) = \sum_{k=0}^{\infty} \left(\frac{\alpha_s(\mu)}{4\pi} \right)^{k+1} \gamma_{\tau=2}^{[J],(k)}$. The leading order expression $\gamma_{\tau=2}^{[J],(0)}$ can be found in [80, 81], while higher-order calculations of $\gamma_{\tau=2}^{[J]}$ and their inverse Mellin transform can be found in [82–90]. Renormalization group invariance implies that

$$\mu \frac{d\bar{D}_N}{d\mu} = -\bar{D}_N \cdot \gamma_{\tau=2}^{[J=N]}. \quad (11)$$

By observing that \bar{D}_N does not depend on Q explicitly, Eq. (9) suggests that one can predict the Q dependence of $\text{ENC}_{1, \Psi_q}^{\text{N.P.}}$ at *fixed* K_\perp solely from the Q dependence of the matrix element of light-ray operators. Specifically, we let $\mu = K_\perp$ in the OPE coefficient, and evolve the matrix element of the light-ray operators from Q to K_\perp using the renormalization group equation (10). Since the physical state $|\Psi_q\rangle$ is μ independent, at fixed K_\perp the Q

dependence of $\text{EEC}_{1,\Psi_q}^{\text{N.P.}}$ is given by

$$\text{ENC}_{1,\Psi_q}^{\text{N.P.}}(K_\perp, Q) = \Lambda_{\text{QCD}} \quad (12)$$

$$\times \bar{D}_N \left(1, \frac{\Lambda_{\text{QCD}}^2}{K_\perp^2} \right) \cdot U_N(K_\perp, Q) \cdot \frac{\langle \bar{\mathcal{O}}_{\tau=2}^{[J=N]}(n; Q) \rangle_{\Psi_q}}{(4\pi)^{-1} \sigma_{\Psi_q} Q^{N-1}},$$

where $U_N(K_\perp, Q)$ is the evolution operator

$$U_N(K_\perp, Q) \equiv \mathbb{P} \exp \left(- \int_{K_\perp}^Q \frac{d\mu}{\mu} \gamma_{\tau=2}^{[J=N]}(\mu) \right). \quad (13)$$

This is one of the main results of this Letter.

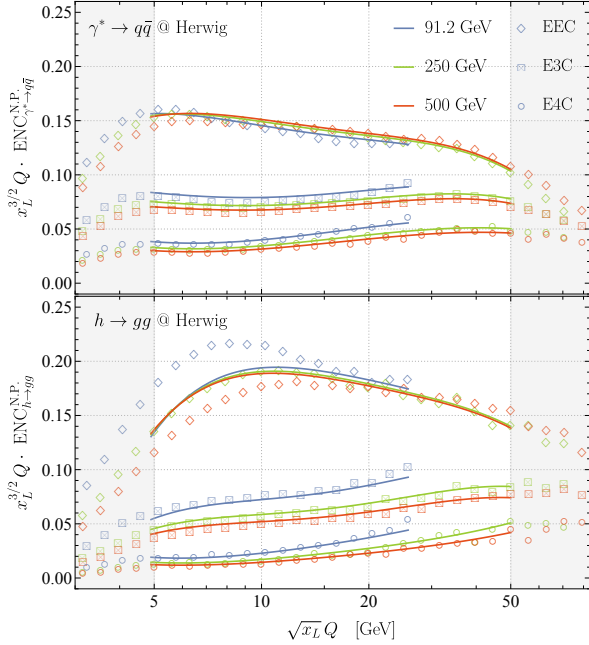


FIG. 3: Comparison of analytic and Monte Carlo predictions for the quantum scaling violation for N -point projected correlators in $\gamma^* \rightarrow q\bar{q}$ and $h \rightarrow gg$.

We finally discuss the implications of Eq. (12) for the factorisation formula of the projected correlator [3, 29]:

$$\text{ENC}_{\Psi_q}(x_L, Q) = \int_0^1 dx \frac{x^N}{x_L} \bar{J}_N \left(\frac{x_L x^2 Q^2}{\mu^2}, \frac{\Lambda_{\text{QCD}}^2}{\mu^2} \right) \cdot \bar{H} \left(x, \frac{Q}{\mu} \right). \quad (14)$$

Based on the equivalence [74] of the light-ray OPE and Eq. (14), we can extend the above factorization formula to include the power corrections derived in this Letter. The hard function \bar{H} encodes the probability of producing a parton with energy fraction x and it corresponds to the normalized matrix element of the twist $\tau = 2$ operators in Eq. (5). The jet function \bar{J}_N is sensitive to the fragmentation at small angular scales and, as such, it encodes also the non-perturbative dynamics. It is mapped [74] onto the OPE coefficients of Eq. (5), from

which we can deduce the following expansion

$$\bar{J}_N \left(\frac{x_L x^2 Q^2}{\mu^2}, \frac{\Lambda_{\text{QCD}}^2}{\mu^2} \right) = \bar{J}_N^{\text{P.T.}} \left(\frac{x_L x^2 Q^2}{\mu^2}, \alpha_s(\mu) \right) + \frac{\Lambda_{\text{QCD}}}{x \sqrt{x_L} Q} \bar{J}_N^{(1)} \left(\frac{x_L x^2 Q^2}{\mu^2}, \frac{\Lambda_{\text{QCD}}^2}{\mu^2} \right) + \dots, \quad (15)$$

where $\bar{J}_N^{\text{P.T.}}$ is the perturbative jet function [3, 21, 29, 49] and $\bar{J}_N^{(1)} = \bar{D}_N|_{K_\perp \rightarrow x K_\perp}$ is the corresponding power correction.

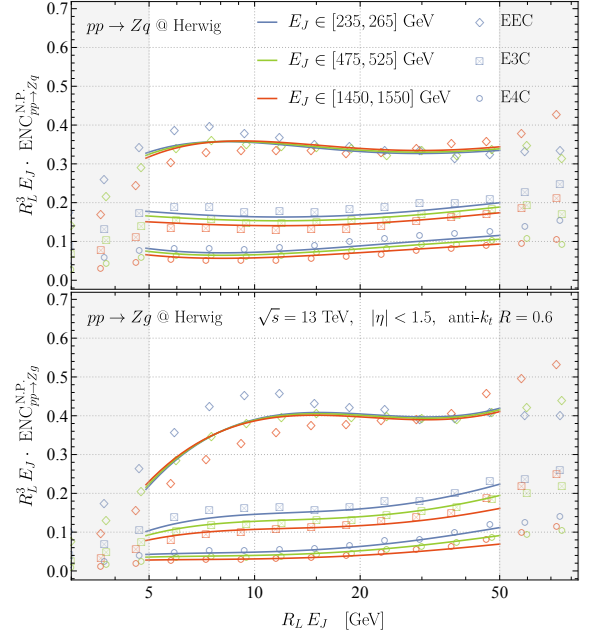


FIG. 4: Comparison of analytic and Monte Carlo predictions for the quantum scaling violation for N -point projected correlators in $pp \rightarrow Zq$ and $pp \rightarrow Zg$.

Monte Carlo validation. — We can now explicitly use Eq. (12) to relate the power correction at a reference scale Q_0 to that at a scale Q . We can express the solution in terms of two non-perturbative functions of K_\perp defining the two components of \bar{D} at a reference scale Q_0 , which can be extracted from the fragmentation of quarks and gluons. At the leading-logarithmic order we find (cf. [77] for details)

$$\begin{pmatrix} \text{ENC}_{1,\gamma^* \rightarrow q\bar{q}}^{\text{N.P.}}(Q) \\ \text{ENC}_{1,h \rightarrow gg}^{\text{N.P.}}(Q) \end{pmatrix}^T = \begin{pmatrix} \text{ENC}_{1,\gamma^* \rightarrow q\bar{q}}^{\text{N.P.}}(Q_0) \\ \text{ENC}_{1,h \rightarrow gg}^{\text{N.P.}}(Q_0) \end{pmatrix}^T \cdot U_N^{\text{LL}}(Q_0, Q), \quad (16)$$

where K_\perp is fixed and kept implicit and $U_N^{\text{LL}}(Q_0, Q) = [\alpha_s(Q)/\alpha_s(Q_0)]^{\gamma_{\tau=2}^{[N],(0)}/(2\beta_0)}$.

We extract the functions $\text{ENC}_{1,\gamma^* \rightarrow q\bar{q}}^{\text{N.P.}}(Q_0)$ and $\text{ENC}_{1,h \rightarrow gg}^{\text{N.P.}}(Q_0)$ from $\gamma^* \rightarrow q\bar{q}$ and $h \rightarrow gg$ at $Q_0 = 250$ GeV for 2-, 3- and 4-point correlators and predict their distribution at a different c.o.m. energy $Q \in$

91.2 – 500 GeV. Specifically, we use events generated with MadGraph5 [91], showered with Herwig 7.2 [92]¹ and analyzed with Rivet [94].² The results are shown in FIG. 3, which displays a comparison of Eq. (16) to the Monte Carlo prediction obtained with Eqs. (7) and (8). We notice that the latter contains subleading power corrections not accounted for in Eq. (16). In general, we observe very good agreement, hence validating the expectation for the perturbative scaling violation presented in this Letter. From FIG. 3 we observe that in the case of the EEC the region of validity of Eq. (16) is substantially pushed towards larger angles. An explanation of this fact, particularly prominent in the gluonic case, is that subleading power corrections neglected in the OPE (3) receive a contribution from operators with $J \sim 1$, whose anomalous dimensions feature a strong enhancement due to the radiation of soft gluons [97–101]. The enhanced quadratic power corrections may be ultimately responsible for the discrepancy in the left region of the plot. This phenomenon is present only in the EEC case while for $N > 2$ the contribution of $J < 2$ operators is further power suppressed.

It is interesting to apply the same procedure to the case of ENC measured on hadronic jets at the LHC [4], in the limit in which the largest angular resolution $\sqrt{x_L} \rightarrow R_L \equiv \sqrt{\Delta y^2 + \Delta \phi^2}$ between detectors is much smaller than the jet radius R . We consider $pp \rightarrow Z + q/g$ jets LHC events at $\sqrt{s} = 13$ TeV, with jet energies in the range $E_J \in 250 - 1500$ GeV. Accordingly we now define $K_\perp = R_L E_J$. Jets are defined using the anti- k_t algorithm [102] with a jet radius $R = 0.6$, as implemented in FastJet [103]. We generate separately events with quark and gluon jets, that we extract from Zq and Zg final states, respectively. An analysis at higher perturbative orders, however, would require a more refined definition of quark and gluon jet fractions. The results are shown in FIG. 4, where the solid lines indicate our predictions from Eq. (16) with $Q_0 = 500$ GeV and $Q = E_J$. The effect of initial-state radiation, present in pp collisions, impacts mildly the correlators measured inside jets at the non-perturbative level (e.g. via colour reconnection). While the EEC, as in FIG. 3, is affected by large subleading power corrections, the analytic prediction describes very

well the simulation for the $N > 2$ correlators, confirming the validity of our results also in the hadron-collider case (cf. [77] for additional studies).

We envision that the leading power correction can be directly extracted from experimental data at a reference scale and then evolved at different scales using the results presented in this letter. In Ref. [77] we present also a study of the effect of quantum scaling violation on ratios of energy correlators, used to measure α_s in Ref. [4]. This work will enhance the role of energy correlators in the precision physics programme and their use for the extraction of fundamental properties of QCD at the LHC and future colliders.

Note added.— While this article was being completed, Ref. [104] presented a related study of the power corrections to the projected correlators using a renormalon analysis in the context of extractions of the strong coupling constant. The connection of their findings to our prediction from the light-ray OPE is non-trivial and deserves further investigation.

ACKNOWLEDGMENTS

We thank Yibei Li, Kyle Lee, Aditya Pathak, David Simmons-Duffin, Iain Stewart, Zhiquan Sun, Gherardo Vita, Xin-Nian Wang and Alexander Zhiboedov for discussions and Silvia Ferrario Ravasio for assistance with the Herwig7 event generator. HC wishes to thank the theory group at CERN for hospitality where this work was initiated. PM wishes to thank the Center for High Energy Physics of Peking University for hospitality while part of this work was carried out. The work of HC, ZX, and HXZ was supported by the National Natural Science Foundation of China (NSFC) under Grant No. 11975200 and No. 12425505. HXZ is also supported by the Startup Grant from Peking University and the Asian Young Scientist Fellowship. The work of PM is funded by the European Union (ERC, grant agreement No. 101044599). Views and opinions expressed are however those of the authors only and do not necessarily reflect those of the European Union or the European Research Council Executive Agency. Neither the European Union nor the granting authority can be held responsible for them.

-
- [1] C. L. Basham, L. S. Brown, S. D. Ellis, and S. T. Love, Phys. Rev. Lett. **41**, 1585 (1978).
 - [2] C. L. Basham, L. S. Brown, S. D. Ellis, and S. T. Love, Phys. Rev. D **19**, 1818 (1979).

- [3] H. Chen, I. Moutl, X. Zhang, and H. X. Zhu, Phys. Rev. D **102**, 054012 (2020), arXiv:2004.11381 [hep-ph].
- [4] A. Hayrapetyan *et al.* (CMS), (2024), arXiv:2402.13864 [hep-ex].
- [5] D. M. Hofman and J. Maldacena, JHEP **05**, 012, arXiv:0803.1467 [hep-th].
- [6] G. P. Korchemsky, JHEP **01**, 008, arXiv:1905.01444 [hep-th].
- [7] M. Kologlu, P. Kravchuk, D. Simmons-Duffin, and A. Zhiboedov, JHEP **01**, 128, arXiv:1905.01311 [hep-th].

¹ Specifically, we use the dot-product preserving shower and corresponding tune from Ref. [93].

² We have repeated the analysis also with Herwig 7.3 [95] and Pythia8 [96], finding consistent results.

- [8] M. Kologlu, P. Kravchuk, D. Simmons-Duffin, and A. Zhiboedov, *JHEP* **11**, 096, arXiv:1904.05905 [hep-th].
- [9] C.-H. Chang, M. Kologlu, P. Kravchuk, D. Simmons-Duffin, and A. Zhiboedov, *JHEP* **05**, 059, arXiv:2010.04726 [hep-th].
- [10] H. Chen, I. Moulton, and H. X. Zhu, *Phys. Rev. Lett.* **126**, 112003 (2021), arXiv:2011.02492 [hep-ph].
- [11] H. Chen, I. Moulton, and H. X. Zhu, *JHEP* **08**, 233, arXiv:2104.00009 [hep-ph].
- [12] C.-H. Chang and D. Simmons-Duffin, *JHEP* **02**, 126, arXiv:2202.04090 [hep-th].
- [13] H. Chen, I. Moulton, J. Sandor, and H. X. Zhu, *JHEP* **09**, 199, arXiv:2202.04085 [hep-ph].
- [14] A. V. Belitsky, S. Hohenegger, G. P. Korchemsky, E. Sokatchev, and A. Zhiboedov, *Phys. Rev. Lett.* **112**, 071601 (2014), arXiv:1311.6800 [hep-th].
- [15] A. V. Belitsky, S. Hohenegger, G. P. Korchemsky, E. Sokatchev, and A. Zhiboedov, *Nucl. Phys. B* **884**, 206 (2014), arXiv:1309.1424 [hep-th].
- [16] A. V. Belitsky, S. Hohenegger, G. P. Korchemsky, E. Sokatchev, and A. Zhiboedov, *Nucl. Phys. B* **884**, 305 (2014), arXiv:1309.0769 [hep-th].
- [17] L. J. Dixon, M.-X. Luo, V. Shtabovenko, T.-Z. Yang, and H. X. Zhu, *Phys. Rev. Lett.* **120**, 102001 (2018), arXiv:1801.03219 [hep-ph].
- [18] H. Chen, M.-X. Luo, I. Moulton, T.-Z. Yang, X. Zhang, and H. X. Zhu, *JHEP* **08** (08), 028, arXiv:1912.11050 [hep-ph].
- [19] J. M. Henn, E. Sokatchev, K. Yan, and A. Zhiboedov, *Phys. Rev. D* **100**, 036010 (2019), arXiv:1903.05314 [hep-th].
- [20] K. Yan and X. Zhang, *Phys. Rev. Lett.* **129**, 021602 (2022), arXiv:2203.04349 [hep-th].
- [21] K. Lee, B. Meçaj, and I. Moulton, (2022), arXiv:2205.03414 [hep-ph].
- [22] T.-Z. Yang and X. Zhang, *JHEP* **09**, 006, arXiv:2208.01051 [hep-ph].
- [23] D. Chicherin, I. Moulton, E. Sokatchev, K. Yan, and Y. Zhu, (2024), arXiv:2401.06463 [hep-th].
- [24] G. P. Korchemsky, E. Sokatchev, and A. Zhiboedov, *JHEP* **08**, 188, arXiv:2106.14899 [hep-th].
- [25] D. Chicherin, G. P. Korchemsky, E. Sokatchev, and A. Zhiboedov, *JHEP* **11**, 134, arXiv:2306.14330 [hep-th].
- [26] C. Csáki and A. Ismail, (2024), arXiv:2403.12123 [hep-ph].
- [27] H. Chen, R. Karlsson, and A. Zhiboedov, (2024), arXiv:2404.15056 [hep-th].
- [28] J. Schwinger, *Proc. Nat. Acad. Sci.* **44**, 956 (1958).
- [29] L. J. Dixon, I. Moulton, and H. X. Zhu, *Phys. Rev. D* **100**, 014009 (2019), arXiv:1905.01310 [hep-ph].
- [30] A. Kardos, S. Kluth, G. Somogyi, Z. Tulipánt, and A. Verbitskyi, *Eur. Phys. J. C* **78**, 498 (2018), arXiv:1804.09146 [hep-ph].
- [31] I. Moulton and H. X. Zhu, *JHEP* **08**, 160, arXiv:1801.02627 [hep-ph].
- [32] A. Gao, H. T. Li, I. Moulton, and H. X. Zhu, *Phys. Rev. Lett.* **123**, 062001 (2019), arXiv:1901.04497 [hep-ph].
- [33] M. A. Ebert, B. Mistlberger, and G. Vita, *JHEP* **08**, 022, arXiv:2012.07859 [hep-ph].
- [34] J. Gao, V. Shtabovenko, and T.-Z. Yang, *JHEP* **02**, 210, arXiv:2012.14188 [hep-ph].
- [35] P. T. Komiske, I. Moulton, J. Thaler, and H. X. Zhu, *Phys. Rev. Lett.* **130**, 051901 (2023), arXiv:2201.07800 [hep-ph].
- [36] J. Holguin, I. Moulton, A. Pathak, and M. Procura, *Phys. Rev. D* **107**, 114002 (2023), arXiv:2201.08393 [hep-ph].
- [37] D. Neill, G. Vita, I. Vitev, and H. X. Zhu, in *Snowmass 2021* (2022) arXiv:2203.07113 [hep-ph].
- [38] H. Chen, I. Moulton, J. Thaler, and H. X. Zhu, *JHEP* **07**, 146, arXiv:2205.02857 [hep-ph].
- [39] L. Ricci and M. Riembau, *Phys. Rev. D* **106**, 114010 (2022), arXiv:2207.03511 [hep-ph].
- [40] E. Craft, K. Lee, B. Meçaj, and I. Moulton, (2022), arXiv:2210.09311 [hep-ph].
- [41] C. Duhr, B. Mistlberger, and G. Vita, *Phys. Rev. Lett.* **129**, 162001 (2022), arXiv:2205.02242 [hep-ph].
- [42] Y. Li, I. Moulton, S. S. van Velzen, W. J. Waalewijn, and H. X. Zhu, *Phys. Rev. Lett.* **128**, 182001 (2022), arXiv:2108.01674 [hep-ph].
- [43] M. Jaarsma, Y. Li, I. Moulton, W. J. Waalewijn, and H. X. Zhu, *JHEP* **12**, 087, arXiv:2307.15739 [hep-ph].
- [44] K. Lee and I. Moulton, (2023), arXiv:2308.00746 [hep-ph].
- [45] Z.-B. Kang, K. Lee, D. Y. Shao, and F. Zhao, *JHEP* **03**, 153, arXiv:2310.15159 [hep-ph].
- [46] H. Cao, H. T. Li, and Z. Mi, *Phys. Rev. D* **109**, 096004 (2024), arXiv:2312.07655 [hep-ph].
- [47] A. Gao, H. T. Li, I. Moulton, and H. X. Zhu, (2023), arXiv:2312.16408 [hep-ph].
- [48] M. Xiao, Y. Ye, and X. Zhu, (2024), arXiv:2405.20001 [hep-ph].
- [49] W. Chen, J. Gao, Y. Li, Z. Xu, X. Zhang, and H. X. Zhu, *JHEP* **05**, 043, arXiv:2307.07510 [hep-ph].
- [50] C. Andres, F. Dominguez, R. Kunnawalkam Elayavalli, J. Holguin, C. Marquet, and I. Moulton, *Phys. Rev. Lett.* **130**, 262301 (2023), arXiv:2209.11236 [hep-ph].
- [51] C. Andres, F. Dominguez, J. Holguin, C. Marquet, and I. Moulton, *JHEP* **09**, 088, arXiv:2303.03413 [hep-ph].
- [52] C. Andres, F. Dominguez, J. Holguin, C. Marquet, and I. Moulton, (2023), arXiv:2307.15110 [hep-ph].
- [53] J. a. Barata, J. G. Milhano, and A. V. Sadofyev, *Eur. Phys. J. C* **84**, 174 (2024), arXiv:2308.01294 [hep-ph].
- [54] Z. Yang, Y. He, I. Moulton, and X.-N. Wang, *Phys. Rev. Lett.* **132**, 011901 (2024), arXiv:2310.01500 [hep-ph].
- [55] J. Holguin, I. Moulton, A. Pathak, M. Procura, R. Schöfbeck, and D. Schwarz, (2023), arXiv:2311.02157 [hep-ph].
- [56] J. a. Barata, P. Caucal, A. Soto-Ontoso, and R. Szafron, (2023), arXiv:2312.12527 [hep-ph].
- [57] X. Liu and H. X. Zhu, *Phys. Rev. Lett.* **130**, 091901 (2023), arXiv:2209.02080 [hep-ph].
- [58] H. Chen, X. Zhou, and H. X. Zhu, *JHEP* **10**, 132, arXiv:2301.03616 [hep-ph].
- [59] H. Cao, X. Liu, and H. X. Zhu, *Phys. Rev. D* **107**, 114008 (2023), arXiv:2303.01530 [hep-ph].
- [60] K. Devereaux, W. Fan, W. Ke, K. Lee, and I. Moulton, (2023), arXiv:2303.08143 [hep-ph].
- [61] X. Liu and H. X. Zhu, (2024), arXiv:2403.08874 [hep-ph].
- [62] A.-P. Chen, X. Liu, and Y.-Q. Ma, (2024), arXiv:2405.10056 [hep-ph].
- [63] K. Konishi, A. Ukawa, and G. Veneziano, *Nucl. Phys. B* **157**, 45 (1979).
- [64] A. Karlberg, G. P. Salam, L. Scyboz, and R. Verheyen, *Eur. Phys. J. C* **81**, 681 (2021), arXiv:2103.16526 [hep-ph].

- [65] M. van Beekveld, M. Dasgupta, B. K. El-Menoufi, J. Helliwell, and P. F. Monni, JHEP **05**, 093, arXiv:2307.15734 [hep-ph].
- [66] G. P. Korchemsky and G. F. Sterman, Nucl. Phys. B **555**, 335 (1999), arXiv:hep-ph/9902341.
- [67] A. V. Belitsky, G. P. Korchemsky, and G. F. Sterman, Phys. Lett. B **515**, 297 (2001), arXiv:hep-ph/0106308.
- [68] S. T. Schindler, I. W. Stewart, and Z. Sun, JHEP **10**, 187, arXiv:2305.19311 [hep-ph].
- [69] Y. L. Dokshitzer, G. Marchesini, and B. R. Webber, JHEP **07**, 012, arXiv:hep-ph/9905339.
- [70] J. D. Bjorken, Phys. Rev. **179**, 1547 (1969).
- [71] G. Altarelli and G. Parisi, Nucl. Phys. B **126**, 298 (1977).
- [72] V. N. Gribov and L. N. Lipatov, Sov. J. Nucl. Phys. **15**, 438 (1972).
- [73] Y. L. Dokshitzer, Sov. Phys. JETP **46**, 641 (1977).
- [74] H. Chen, JHEP **01**, 035, arXiv:2311.00350 [hep-ph].
- [75] N. A. Sveshnikov and F. V. Tkachov, Phys. Lett. B **382**, 403 (1996), arXiv:hep-ph/9512370.
- [76] P. Kravchuk and D. Simmons-Duffin, JHEP **11**, 102, arXiv:1805.00098 [hep-th].
- [77] H. Chen, P. Monni, Z. Xu, and H. X. Zhu, Supplemental material to this letter (2024).
- [78] Y. L. Dokshitzer, G. Marchesini, and B. R. Webber, Nucl. Phys. B **469**, 93 (1996), arXiv:hep-ph/9512336.
- [79] S. Caron-Huot, M. Kologlu, P. Kravchuk, D. Meltzer, and D. Simmons-Duffin, JHEP **04**, 014, arXiv:2209.00008 [hep-th].
- [80] D. J. Gross and F. Wilczek, Phys. Rev. D **9**, 980 (1974).
- [81] D. J. Gross and F. Wilczek, Phys. Rev. D **8**, 3633 (1973).
- [82] S. Moch, J. A. M. Vermaseren, and A. Vogt, Nucl. Phys. B **688**, 101 (2004), arXiv:hep-ph/0403192.
- [83] A. Vogt, S. Moch, and J. A. M. Vermaseren, Nucl. Phys. B **691**, 129 (2004), arXiv:hep-ph/0404111.
- [84] H. Chen, T.-Z. Yang, H. X. Zhu, and Y. J. Zhu, Chin. Phys. C **45**, 043101 (2021), arXiv:2006.10534 [hep-ph].
- [85] J. Blümlein, P. Marquard, C. Schneider, and K. Schönwald, Nucl. Phys. B **971**, 115542 (2021), arXiv:2107.06267 [hep-ph].
- [86] T. Gehrmann, A. von Manteuffel, V. Sotnikov, and T.-Z. Yang, Phys. Lett. B **849**, 138427 (2024), arXiv:2310.12240 [hep-ph].
- [87] S. Moch, B. Ruijl, T. Ueda, J. A. M. Vermaseren, and A. Vogt, Phys. Lett. B **825**, 136853 (2022), arXiv:2111.15561 [hep-ph].
- [88] G. Falcioni, F. Herzog, S. Moch, and A. Vogt, Phys. Lett. B **842**, 137944 (2023), arXiv:2302.07593 [hep-ph].
- [89] G. Falcioni, F. Herzog, S. Moch, and A. Vogt, Phys. Lett. B **846**, 138215 (2023), arXiv:2307.04158 [hep-ph].
- [90] G. Falcioni, F. Herzog, S. Moch, A. Pelloni, and A. Vogt, (2024), arXiv:2404.09701 [hep-ph].
- [91] J. Alwall, M. Herquet, F. Maltoni, O. Mattelaer, and T. Stelzer, JHEP **06**, 128, arXiv:1106.0522 [hep-ph].
- [92] J. Bellm *et al.*, Eur. Phys. J. C **80**, 452 (2020), arXiv:1912.06509 [hep-ph].
- [93] G. Bewick, S. Ferrario Ravasio, P. Richardson, and M. H. Seymour, JHEP **04**, 019, arXiv:1904.11866 [hep-ph].
- [94] C. Bierlich *et al.*, SciPost Phys. **8**, 026 (2020), arXiv:1912.05451 [hep-ph].
- [95] G. Bewick *et al.*, (2023), arXiv:2312.05175 [hep-ph].
- [96] T. Sjöstrand, S. Ask, J. R. Christiansen, R. Corke, N. Desai, P. Ilten, S. Mrenna, S. Prestel, C. O. Ras-
- mussen, and P. Z. Skands, Comput. Phys. Commun. **191**, 159 (2015), arXiv:1410.3012 [hep-ph].
- [97] L. N. Lipatov, Phys. Rept. **286**, 131 (1997), arXiv:hep-ph/9610276.
- [98] R. C. Brower, J. Polchinski, M. J. Strassler, and C.-I. Tan, JHEP **12**, 005, arXiv:hep-th/0603115.
- [99] T. Jaroszewicz, Phys. Lett. B **116**, 291 (1982).
- [100] A. V. Kotikov and L. N. Lipatov, Nucl. Phys. B **582**, 19 (2000), arXiv:hep-ph/0004008.
- [101] A. V. Kotikov and L. N. Lipatov, Nucl. Phys. B **661**, 19 (2003), [Erratum: Nucl.Phys.B 685, 405–407 (2004)], arXiv:hep-ph/0208220.
- [102] M. Cacciari, G. P. Salam, and G. Soyez, JHEP **04**, 063, arXiv:0802.1189 [hep-ph].
- [103] M. Cacciari, G. P. Salam, and G. Soyez, Eur. Phys. J. C **72**, 1896 (2012), arXiv:1111.6097 [hep-ph].
- [104] K. Lee, A. Pathak, I. Stewart, and Z. Sun, (2024), arXiv:2405.19396 [hep-ph].

SUPPLEMENTAL MATERIAL

1. ENC measured in jets in $\gamma^* \rightarrow q\bar{q}$ and $h \rightarrow gg$

In this appendix we repeat the analysis shown in the main text for the case of ENC measured inside jets produced in the decays $\gamma^* \rightarrow q\bar{q}$ and $h \rightarrow gg$. For consistency with the $pp \rightarrow Z + \text{jets}$ case shown in FIG. 4, we consider the e^+e^- version of the anti- k_t algorithm, belonging to the family of generalized k_t algorithms in Ref. [103], with $R = 0.6$, and denote the largest angular distance by $R_L \ll R$.

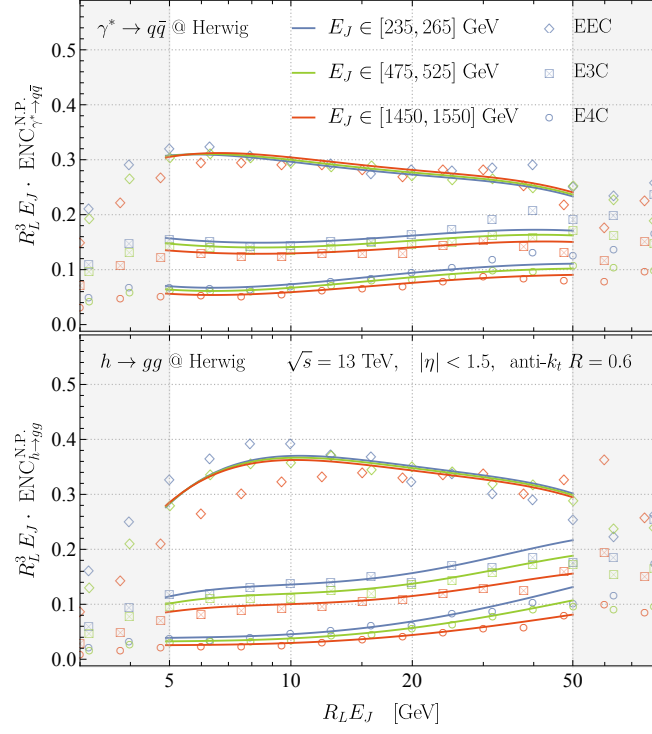


FIG. 5: Comparison of analytic and Monte Carlo predictions for the quantum scaling violation for N -point projected correlators measured in jets in $\gamma^* \rightarrow q\bar{q}$ and $h \rightarrow gg$.

The non-perturbative boundary conditions are extracted at $Q_0 = 500$ GeV and then Eq. (16) is used to predict the power corrections in the range $E_J \in 250 - 1500$ GeV. The results are summarised in FIG. 5. When compared to FIG. 4, we observe a better agreement between the analytic prediction and the Monte Carlo data for the fermionic final state. This is due to the absence of initial-state radiation, which in FIG. 4 introduces an additional source of non-perturbative correlation with the radiation within the jet. The description of Monte Carlo data is somewhat less good in the right region of the plot, where effects due to the finite size of the jet play a role.

2. Properties of Light-ray Operators and ansatz for the Light-ray OPE

In this appendix we elaborate on the *classical* symmetry properties of light-ray operators and their guidance to build a general light-ray OPE ansatz for non-perturbative power corrections. We discuss the case of $d = 4$ spacetime dimensions, but the generalization to other spacetime dimensions is straightforward.

Let us consider a light-ray operator $\mathbb{O}_\tau^{[J]}$ as the light transform of the corresponding local operator $\mathcal{O}_\tau^{[J]}(x; \bar{n}) = \mathcal{O}_\tau^{\mu_1 \dots \mu_J}(x) \bar{n}_{\mu_1} \dots \bar{n}_{\mu_J}$

$$\mathbb{O}_\tau^{[J]}(n) = \mathbb{L}_\tau[\mathcal{O}_\tau^{[J]}(x; \bar{n})|_{x=(t, r\bar{n})}] = \lim_{r \rightarrow \infty} r^\tau \int_0^\infty dt \mathcal{O}_\tau^{[J]}(x; \bar{n})|_{x=(t, r\bar{n})}, \quad (\text{S.1})$$

where we define two null vectors $n^\mu = (1, \vec{n})$, $\bar{n}^\mu = (1, -\vec{n})$. The local operator $\mathcal{O}_\tau^{[J]}(x; \bar{n})$ has dimension $\Delta = \tau + J$ and the light transform operator \mathbb{L}_τ carries dimension $-(1 + \tau)$, which leads to the fact that the light-ray operator

$\mathbb{O}_\tau^{[J]}(n)$ has dimension $J - 1$. The collinear spin is associated with Lorentz boosts along \vec{n} . To count the collinear spin, we choose the convention to assign n^μ with collinear spin $+1$, and \bar{n}^μ with -1 . To associate a collinear spin to the light transform operation, we rewrite it in terms of light-cone coordinates

$$\mathbb{L}_\tau = \lim_{\vec{n} \cdot x \rightarrow \infty} \left(\frac{\vec{n} \cdot x}{2} \right)^\tau \int_{-\infty}^{\infty} d(n \cdot x), \quad (\text{S.2})$$

from which we can directly identify the collinear spin to be $1 - \tau$. Since the local operator $\mathcal{O}_\tau^{[J]}(x; \vec{n})$ carries collinear spin $-J$, the collinear spin of the light-ray operator $\mathbb{O}_\tau^{[J]}(n)$ is $1 - (\tau + J)$.

One reason to discuss dimension and collinear spin is that the expansion parameters $\zeta_{ij} = \frac{n_i \cdot n_j}{2}$ and $x_L = \max \zeta_{ij}$ in the small angle limit are dimensionless and have nice transformation properties under boost. Assume we make an infinitesimal boost transformation along \vec{n} . The unit vectors \vec{n}_i on the celestial sphere change in the following way

$$\vec{n}_i \rightarrow \vec{n}_i + \epsilon(\vec{n} - (\vec{n} \cdot \vec{n}_i)\vec{n}_i), \quad (\text{S.3})$$

where ϵ is the infinitesimal parameter of the boost transformation. This leads to the transformation of ζ_{ij}

$$\zeta_{ij} \rightarrow (1 - \epsilon(\vec{n} \cdot \vec{n}_i + \vec{n} \cdot \vec{n}_j))\zeta_{ij} \approx (1 - 2\epsilon)\zeta_{ij}, \quad (\text{S.4})$$

where we have used the collinear approximation $\vec{n} \cdot \vec{n}_i \approx \vec{n} \cdot \vec{n}_j \approx 1$ in the second step. This means that the Lorentz boost acts as a dilation on the celestial sphere. As suggested by the coefficient of ϵ , in the collinear limit, ζ_{ij} and x_L carry weight 2 under a boost transformation.

Now let us consider the collinear limit $n_i \rightarrow n$ for the product of N energy flow operators in terms of light-ray OPE

$$\lim_{n_i \rightarrow n} \mathcal{E}(n_1) \cdots \mathcal{E}(n_N) \supset \Lambda_{\text{QCD}}^\alpha \mathcal{C}_{\alpha, \tau, J}(\{\zeta_{ij}\}) \mathbb{O}_\tau^{[J]}(n), \quad (\text{S.5})$$

where we consider the OPE coefficient with dimension α , with $\mathcal{C}_{\alpha, \tau, J}$ being a dimensionless function. The l.h.s. of (S.5) has dimension N , while the r.h.s. has the dimension $\alpha + (J - 1)$. Balancing the dimension on both sides fixes the label J to be

$$J = N + 1 - \alpha. \quad (\text{S.6})$$

Note that the energy flow operator \mathcal{E} has the labels $\tau = 2$, $J = 2$ and hence has collinear spin -3 . In the collinear limit, the collinear spin of (S.5) on the l.h.s. is then $-3N$ and the collinear spin of $\mathbb{O}_\tau^{[J=N+1-\alpha]}(n)$ is $\alpha - \tau - N$. This requires that the coefficient function $\mathcal{C}_{\alpha, \tau, J=N+1-\alpha}(\{\zeta_{ij}\})$ has collinear spin $\tau - 2N - \alpha$, that is

$$\mathcal{C}_{\alpha, \tau, J=N+1-\alpha}(\{\zeta_{ij}\}) = \frac{1}{x_L^{(\alpha+2N-\tau)/2}} \tilde{\mathcal{C}}_{\alpha, \tau, J=N+1-\alpha}(\{\zeta_{ij}/x_L\}), \quad (\text{S.7})$$

where we have factored out the overall x_L dependence and $\tilde{\mathcal{C}}_{\alpha, \tau, J=N+1-\alpha}(\{\zeta_{ij}/x_L\})$, carrying the information of the shape dependence on the N -point configuration, then has collinear spin 0. For projected N -point energy correlators, additional integrations over the angular variables will introduce x_L dependence due to the boundary constraint $x_L = \max \zeta_{ij}$. Without loss of generality, let us assume $x_L = \zeta_{12}$ and evaluate the remaining $N - 2$ angular integrals with the measure $d^2 \vec{n}_3 \cdots d^2 \vec{n}_N$. Working out the explicit Jacobian from the change of measure is not easy, but the overall scaling with respect to x_L is straightforward

$$\int_{\zeta_{ij} \leq x_L} d^2 \vec{n}_3 \cdots d^2 \vec{n}_N \sim x_L^{N-2}. \quad (\text{S.8})$$

Therefore, we obtain the following ansatz for a term of dimension α contributing to the light-ray OPE

$$\int d\Omega \lim_{n_i \rightarrow n} \mathcal{E}(n_1) \cdots \mathcal{E}(n_N) \supset \Lambda_{\text{QCD}}^\alpha \frac{D_{N, \tau}^{(\alpha)}}{x_L^{(\alpha-\tau)/2+2}} \mathbb{O}_\tau^{[J=N+1-\alpha]}(n), \quad (\text{S.9})$$

where the coefficient $D_{N, \tau}^{(\alpha)}$ is related to $\tilde{\mathcal{C}}_{\alpha, \tau, J=N+1-\alpha}(\{\zeta_{ij}/x_L\})$ by integrating out all the shape dependence.

Eq. (S.9) shows that the expansion in the collinear limit is controlled by the twist of light-ray operators. In perturbative QCD, the leading twist is 2 in which the classical degeneracy of quark and gluon twist-2 operators

occurs. We can now neglect, in good approximation, the contribution from higher twist operators to the collinear limit and we obtain the following form for the leading twist light-ray OPE

$$\int d\Omega \lim_{n_i \rightarrow n} \mathcal{E}(n_1) \cdots \mathcal{E}(n_N) = \int_0^{N-\epsilon} d\alpha \frac{\Lambda_{\text{QCD}}^\alpha}{x_L^{1+\alpha/2}} \vec{D}_{N,\tau=2}^{(\alpha)} \cdot \vec{\mathbb{O}}_{\tau=2}^{[J=N+1-\alpha]}(n) + o(\Lambda_{\text{QCD}}^{N-\epsilon}) + \text{higher twists}, \quad (\text{S.10})$$

where the integral over the dimension parameter α indicates that all twist-2 light-ray operators can in principle appear in the light-ray OPE. We introduce a small positive parameter $\epsilon > 0$ to avoid the complication of non-DGLAP evolution when the label $J \sim 1$ [97–101]. The perturbative result corresponds to the case where $\vec{D}_{N,\tau=2}^{(\alpha)}$ behaves like $\delta(\alpha)$ and its derivatives near $\alpha \sim 0$ [74]. In Eqs. (3) and (5), we supplement Eq. (S.10) with the assumption that the leading power correction is of order $\mathcal{O}(\Lambda_{\text{QCD}})$, which translates to the condition that $\vec{D}_{N,\tau=2}^{(\alpha)}$ has localized distributions at $\alpha = 1$, such as $\delta(\alpha - 1)$. The linearity assumption is backed by explicit calculations in various non-perturbative models [2, 66–68, 78], that we have verified with an explicit calculation in the dispersive approach of Ref. [78].

The power of the light-ray OPE (S.10) is that it allows us to gain an understanding of the collinear parametrization beyond first the power correction as well as of their quantum evolution giving rise to the quantum scaling violation.

From (S.10), we can qualitatively infer the reason why our prediction for the evolution of the leading power correction does not describe very well the EEC data while providing a good description for the higher-point projective correlators (see FIG. 3). In the EEC case, the leading power correction consists of $J = 2$ operators, whose anomalous dimension matrix $\gamma_{\tau=2}^{[J=2]}$ contains one vanishing eigenvalue. This explains the reason why the leading power correction has a very moderate scale evolution. On the other hand, the subleading contributions of order $\mathcal{O}(\Lambda_{\text{QCD}}^{(\alpha \approx 2)})$ are sensitive to the $J = 1$ pole in the anomalous dimensions, thus they are expected to have larger scaling evolution effects and require BFKL resummation when the label J is very close to 1 [97–101]. However, for $N \geq 3$ the evolution of the next few subleading-power corrections is milder than that in the leading power correction because the eigenvalues of $\gamma_{\tau=2}^{[J>2]}$ are positive and monotonically increasing with J . In these cases, the subtleties due to the $J = 1$ pole are delayed to higher power corrections.

3. Leading Logarithmic Approximation

In this section, we discuss the calculation of the leading power correction quantities $\text{ENC}_1^{\text{N.P.}}(K_\perp, Q)$ for various states $\{|\Psi_q\rangle\}$ and energy scales $\{Q\}$ at Leading-Logarithmic (LL) accuracy³. The starting point is Eq. (9) and we set the factorization scale $\mu = K_\perp$

$$\text{ENC}_1^{\text{N.P.}}(K_\perp, Q) = \Lambda_{\text{QCD}} \vec{D}_N \left(1, \frac{\Lambda_{\text{QCD}}^2}{K_\perp^2}\right) \cdot \left[\frac{\langle \vec{\mathbb{O}}_{\tau=2}^{[J=N]}(n; \mu) \rangle_{\Psi_q}}{(4\pi)^{-1} \sigma_{\Psi_q} Q^{N-1}} \left(\frac{Q^2}{\mu^2}\right) \right] \Big|_{\mu=K_\perp}.$$

Assuming that the state $|\Psi_q\rangle$ is physical and hence it does not depend on the factorization scale μ , the light-ray operator renormalization equation (10) gives the corresponding evolution equation for the matrix element

$$\mu \frac{d}{d\mu} \langle \vec{\mathbb{O}}_{\tau=2}^{[J]}(n; \mu) \rangle_{\Psi_q} = \gamma_{\tau=2}^{[J]}(\mu) \cdot \langle \vec{\mathbb{O}}_{\tau=2}^{[J]}(n; \mu) \rangle_{\Psi_q}, \quad (\text{S.11})$$

whose solution can be generated by the evolution operator in (13)

$$\langle \vec{\mathbb{O}}_{\tau=2}^{[J]}(n; \mu) \rangle_{\Psi_q} = U_N(\mu, Q) \cdot \langle \vec{\mathbb{O}}_{\tau=2}^{[J]}(n; Q) \rangle_{\Psi_q}. \quad (\text{S.12})$$

This leads to the main result in the Letter (12). In the LL approximation, the evolution matrix is determined by the leading-order anomalous dimension matrix $\gamma_{\tau=2}^{[J]}(\mu) = \frac{\alpha_s(\mu)}{4\pi} \gamma_{\tau=2}^{[J],(0)} + \mathcal{O}(\alpha_s^2)$ and $\gamma_{\tau=2}^{[J],(0)}$ is [80, 81]

$$\gamma_{\tau=2}^{[J],(0)} = \begin{pmatrix} 2C_F(4H_J - \frac{2}{J(J+1)} - 3) & -T_F \frac{4(J^2+J+2)}{J(J+1)(J+2)} \\ -C_F \frac{4(J^2+J+2)}{(J-1)J(J+1)} & 8C_A(H_J - \frac{2(J^2+J+1)}{(J-1)J(J+1)(J+2)}) - 2\beta_0 \end{pmatrix}, \quad (\text{S.13})$$

³ When presenting the light-ray OPE method, Eq. (9) is the result of a simplified calculation at leading-logarithmic accuracy. On the other hand, the factorization formula (14) extends to all logarithmic orders where the variable x inside the jet function plays a very important role. This requires including derivatives of light-ray operators in the light-ray OPE. For technical details, one can follow Ref. [74] to generalize (9) to all logarithmic orders, which will be equivalent to the factorization formula (14).

where $H_J = \sum_{n=1}^J \frac{1}{n}$ is the harmonic number, $\beta_0 = \frac{11}{3}C_A - \frac{4}{3}n_f T_F$ is the one-loop QCD beta function. The path ordering exponential in (13) simplifies at LL and gives

$$U_N^{\text{LL}}(K_\perp, Q) = \left[\frac{\alpha_s(Q)}{\alpha_s(K_\perp)} \right]^{\gamma_{\tau=2}^{[N],(0)}/(2\beta_0)}. \quad (\text{S.14})$$

The matrix element $\langle \vec{\mathcal{O}}_{\tau=2}^{[J]}(n; Q) \rangle_{\Psi_q}$ can be approximated by the perturbative result because we work under the assumption of the hierarchy $Q \gg \Lambda_{\text{QCD}}$. Further hadronization corrections to this matrix element are not enhanced in the collinear limit and hence can be neglected. In the LL approximation, we only need the leading-order contribution in the process-dependent quantity $\frac{\langle \vec{\mathcal{O}}_{\tau=2}^{[J=N]}(n_k; Q) \rangle_{\Psi_q}}{(4\pi)^{-1} \sigma_{\Psi_q} Q^{N-1}}$. This is $(2^{2-N}, 0)^T + \mathcal{O}(\alpha_s)$ for $\gamma^* \rightarrow q\bar{q}$ and $(0, 2^{2-N})^T + \mathcal{O}(\alpha_s)$ for $h \rightarrow gg$, from which we can extract out the quark jet and gluon jet leading non-perturbative correction functions, respectively. We now denote all parts in the r.h.s. of Eq. (12) independent of the state $|\Psi_q\rangle$ (when Q is fixed) as $\vec{F}_1^{[N]}(K_\perp, Q)$:

$$\vec{F}_1^{[N]}(K_\perp, Q) \equiv \Lambda_{\text{QCD}} \vec{D}_N \left(1, \frac{\Lambda_{\text{QCD}}^2}{K_\perp^2} \right) \cdot U_N(K_\perp, Q). \quad (\text{S.15})$$

This vector contains the information of the quark and gluon leading non-perturbative functions as well as the perturbative scale evolution. From the definition (S.15), we can find that $\vec{F}_1^{[N]}$ evolves as follows between two scales Q and Q_0

$$\vec{F}_1^{[N]}(K_\perp, Q) = \vec{F}_1^{[N]}(K_\perp, Q_0) \cdot U_N(Q_0, Q). \quad (\text{S.16})$$

The LL predictions for $\gamma^* \rightarrow q\bar{q}$ and $h \rightarrow gg$ are then

$$\text{ENC}_{1, \gamma^* \rightarrow q\bar{q}}^{\text{N.P.}}(K_\perp, Q) = \vec{F}_1^{[N]}(K_\perp, Q) \cdot \begin{pmatrix} 2^{2-N} \\ 0 \end{pmatrix}, \quad (\text{S.17})$$

$$\text{ENC}_{1, h \rightarrow gg}^{\text{N.P.}}(K_\perp, Q) = \vec{F}_1^{[N]}(K_\perp, Q) \cdot \begin{pmatrix} 0 \\ 2^{2-N} \end{pmatrix}, \quad (\text{S.18})$$

from which we can deduce the following LL relation

$$\begin{pmatrix} \text{ENC}_{1, \gamma^* \rightarrow q\bar{q}}^{\text{N.P.}}(K_\perp, Q) \\ \text{ENC}_{1, h \rightarrow gg}^{\text{N.P.}}(K_\perp, Q) \end{pmatrix}_{\text{LL}}^T = \begin{pmatrix} \text{ENC}_{1, \gamma^* \rightarrow q\bar{q}}^{\text{N.P.}}(K_\perp, Q_0) \\ \text{ENC}_{1, h \rightarrow gg}^{\text{N.P.}}(K_\perp, Q_0) \end{pmatrix}_{\text{LL}}^T \cdot U_N^{\text{LL}}(Q_0, Q). \quad (\text{S.19})$$

Similarly, we obtain a similar relation for quark and gluon jets in the $pp \rightarrow Z + \text{jet}$ case

$$\begin{pmatrix} \text{ENC}_{1, pp \rightarrow Zq}^{\text{N.P.}}(K_\perp, E_J) \\ \text{ENC}_{1, pp \rightarrow Zg}^{\text{N.P.}}(K_\perp, E_J) \end{pmatrix}_{\text{LL}}^T = \begin{pmatrix} \text{ENC}_{1, pp \rightarrow Zq}^{\text{N.P.}}(K_\perp, E_{J,0}) \\ \text{ENC}_{1, pp \rightarrow Zg}^{\text{N.P.}}(K_\perp, E_{J,0}) \end{pmatrix}_{\text{LL}}^T \cdot U_N^{\text{LL}}(E_{J,0}, E_J), \quad (\text{S.20})$$

where E_J is the jet energy and we have used $K_\perp = R_L E_J$ as in the Letter. The validation of these relations are described in the section *Monte Carlo validation*.

4. Different strategies to predict scaling violation and subleading power corrections

We now discuss the extraction of the non-perturbative boundary conditions to Eq. (S.22) that fix the two entries of the vector \vec{D} . We can take two strategies, discussed in the following.

The first strategy is to extract the two non-perturbative entries of \vec{D} at a fixed energy $Q = Q_0$, using both quark and gluon data (for instance via the $\gamma^* \rightarrow q\bar{q}$ and $h \rightarrow gg$ decays). This is the strategy adopted in the Letter, and resulting in the predictions shown in FIG. 3 and FIG. 4. The advantage of this strategy is that it extracts simultaneously quark and gluon distributions. Moreover, this allows us to target more precisely the leading power correction $\mathcal{O}(\Lambda_{\text{QCD}}/Q)$ provided the scale K_\perp is sufficiently large.

The second strategy is instead to use either only quark or only gluon data at *two* different energies Q_1 and Q_2 . One advantage of using two different energy scales is that this strategy partly captures subleading power corrections, and hence it is expected to work better at lower energies as well as in the EEC case, for which we have found that

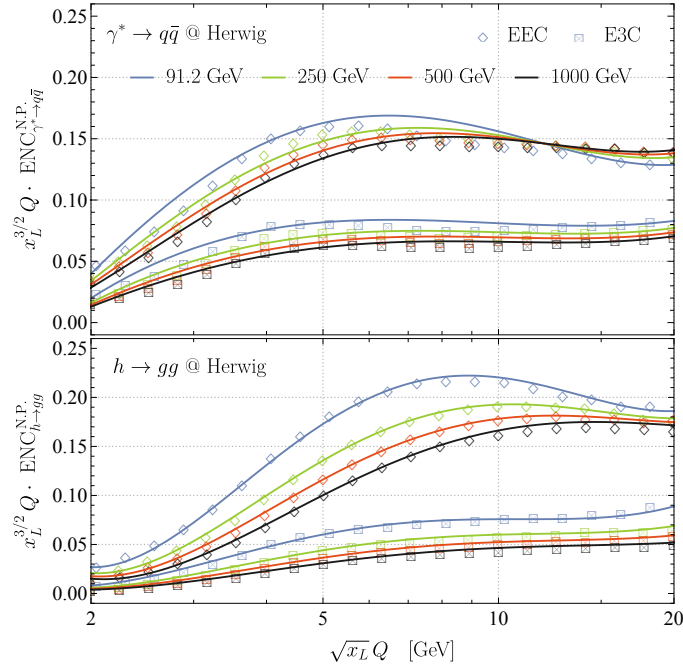


FIG. 6: Comparison of approximate relation (S.25) and Monte Carlo predictions for the quantum scaling violation for N -point projected correlators in $\gamma^* \rightarrow q\bar{q}$ and $h \rightarrow gg$. The 250 GeV curves (green) and the 500 GeV curves (red) are extracted from Monte Carlo data, while the 91.2 GeV curves (blue) and the 1000 GeV curves (black) are predictions from (S.25).

higher power corrections are enhanced (cf. FIG. 3). On the other hand, one disadvantage is that it cannot be used to extract, simultaneously, the quark and gluon distributions since we only have two degrees of freedom. To show how to implement this, we can diagonalize the LL kernel (S.14) using the right eigenvectors of $\gamma_{\tau=2}^{[N],(0)}$

$$\gamma_{\tau=2}^{[N],(0)} \cdot \vec{v}_i^{[N]} = \lambda_i^{[N]} \vec{v}_i^{[N]}, \quad (\text{S.21})$$

where $\lambda_{i=1,2}^{[N]}$ is the eigenvalue corresponding to i -th right eigenvector $\vec{v}_i^{[N]}$. As a result, the LL approximation for Eq. (S.15) becomes

$$\vec{F}_1^{[N]}(K_\perp, Q) \cdot \vec{v}_i^{[N]} = \left[\frac{\alpha_s(Q)}{\alpha_s(K_\perp)} \right]^{\lambda_i^{[N]}/(2\beta_0)} \left[\Lambda_{\text{QCD}} \vec{D}_N \left(1, \frac{\Lambda_{\text{QCD}}^2}{K_\perp^2} \right) \cdot \vec{v}_i^{[N]} \right]. \quad (\text{S.22})$$

From Eq. (S.22) we can establish the relation

$$\vec{F}_1^{[N]}(K_\perp, Q) = \frac{R_N(Q, Q_2)}{R_N(Q_1, Q_2)} \vec{F}_1^{[N]}(K_\perp, Q_1) + \frac{R_N(Q_1, Q)}{R_N(Q_1, Q_2)} \vec{F}_1^{[N]}(K_\perp, Q_2), \quad (\text{S.23})$$

where R_N is defined as the determinant

$$R_N(Q_1, Q_2) = \det \begin{pmatrix} \alpha_s(Q_1)^{\lambda_1^{[N]}/(2\beta_0)} & \alpha_s(Q_1)^{\lambda_2^{[N]}/(2\beta_0)} \\ \alpha_s(Q_2)^{\lambda_1^{[N]}/(2\beta_0)} & \alpha_s(Q_2)^{\lambda_2^{[N]}/(2\beta_0)} \end{pmatrix}. \quad (\text{S.24})$$

It turns out that ratios of R functions in Eq. (S.23) is numerically not very sensitive to the value of anomalous dimensions or N . Therefore, such a relation may numerically, and approximately, capture terms beyond the leading power correction because we expect that the next few contributions are described by the anomalous dimensions at nearby $J < N$. This leads to the approximate relation

$$x_L^{3/2} Q \text{ENC}_{\Psi_q}^{\text{N.P.}}(K_\perp, Q) \approx \frac{R_N(Q, Q_2)}{R_N(Q_1, Q_2)} x_L^{3/2} Q_1 \text{ENC}_{\Psi_q}^{\text{N.P.}}(K_\perp, Q_1) + \frac{R_N(Q_1, Q)}{R_N(Q_1, Q_2)} x_L^{3/2} Q_2 \text{ENC}_{\Psi_q}^{\text{N.P.}}(K_\perp, Q_2), \quad (\text{S.25})$$

which provides reliable predictions over a wider range of K_\perp near the transition region. We show the results of this procedure applied separately to quark and gluon final states in FIG. 6. Here we choose $Q_1 = 250$ GeV, $Q_2 = 500$ GeV, and generate Monte Carlo data for both $\gamma^* \rightarrow q\bar{q}$ and $h \rightarrow gg$ processes as input, and make predictions at $Q = \{91.2, 1000\}$ GeV. We see that this procedure leads to a very good description of the data in the region $\sqrt{x_L}Q \lesssim 15$ GeV where leading power correction predictions fail in EEC, indicating that (S.25) could approximately capture also the evolution of the subleading power corrections.

An important aspect of FIG. 6 is that quark and gluon distributions are extracted separately, that is we extract four non-perturbative distributions rather than the usual two used in Eq. (16). This clearly makes it impossible to describe quark and gluon data with a single set of non-perturbative functions of K_\perp . A rigorous way of dealing with this problem would be to consider the consistent inclusion of subleading power corrections in the OPE.

5. Impact of quantum scaling violation on ratios of energy correlators

In the Letter we have shown that the dominant classical scaling of the power corrections to energy correlators receives a correction due to quantum scaling violation. Although the latter is numerically subdominant at the level of the individual correlator, its effect is instrumental when one considers ratios of correlators [3] such as E3C/EEC. The measurement of ratios of this type has been used for recent extractions of the strong coupling constant by the CMS collaboration [4].

In this section we discuss the impact of quantum scaling violation on the ratio of energy correlators ENC/EEC. Explicitly, we define the non-perturbative correction to such ratios as

$$R_\Psi^{\text{N.P., } N/2}(x_L, Q) \equiv \left[\frac{\text{ENC}_\Psi(x_L, Q)}{\text{EEC}_\Psi(x_L, Q)} \right]^{\text{Hadron}} - \left[\frac{\text{ENC}_\Psi(x_L, Q)}{\text{EEC}_\Psi(x_L, Q)} \right]^{\text{Parton}}, \quad (\text{S.26})$$

where as usual $\Psi = \{\gamma^* \rightarrow q\bar{q}, h \rightarrow gg\}$ denotes the specific final state in which the correlator is measured.

We explicitly consider the ratio E3C/EEC, whose power corrections are shown in Fig. 7 for $\gamma^* \rightarrow q\bar{q}$ (left plot) and $h \rightarrow gg$ (right plot). The dominant effect due to classical scaling largely cancels at the level of the ratio, hence enhancing the effect of quantum scaling violation. In the figures, the latter effect is responsible for the spread between data at different collision energies, which is not predicted by the classical scaling (i.e. all curves would be otherwise completely overlapping). Therefore the effect of quantum scaling is substantial at the level of the ratios, hence playing a significant role in experimental extractions of the strong coupling constant.

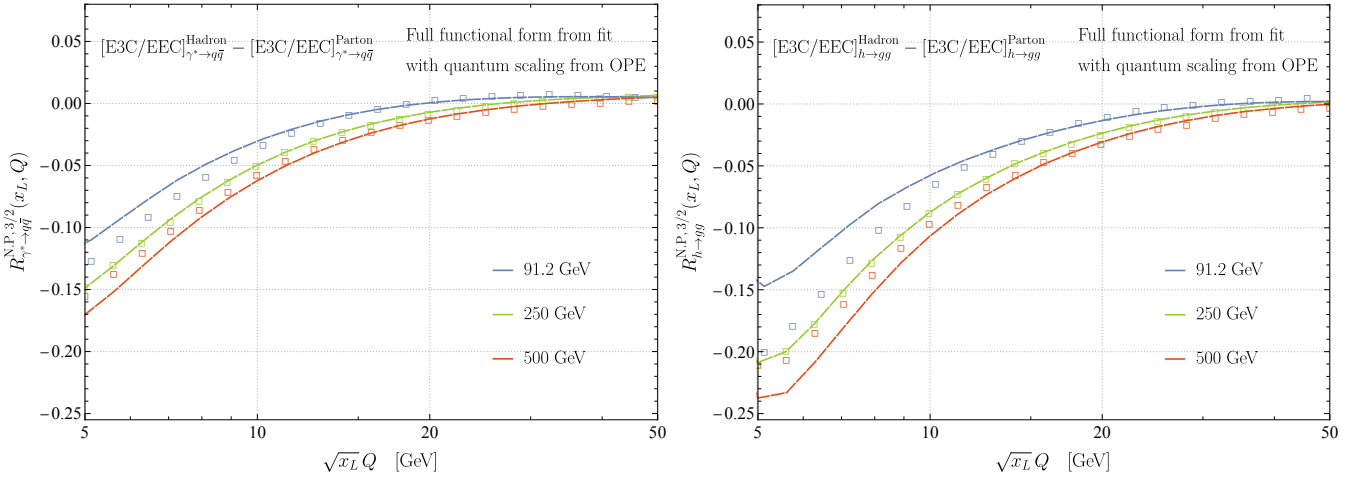


FIG. 7: Leading power correction for the ratio E3C/EEC measured in $\gamma^* \rightarrow q\bar{q}$ (left) and $h \rightarrow gg$ (right). The solid lines represent the predictions from the quantum scaling violation derived in the Letter, where the non-perturbative function of $\sqrt{x_L}Q$ is obtained from a fit of Monte Carlo data $Q = 250$ GeV and then evolved using the evolution equation given in the Letter. The squares are the result of Monte Carlo simulations.

As done in the main text, we compare our prediction for the leading power correction to a Monte Carlo simulation obtained with Herwig 7.2, for both quark and gluon processes. The Monte Carlo data are represented by the squares, while the lines represent our prediction. To obtain that, we fit the non-perturbative $\sqrt{x_L}Q$ dependence at the reference

energy $Q = 250$ GeV, and then evolve in Q using the results of the Letter. As it can be seen from Fig. 7 the evolution of the quantum scaling leads to a rather good description of the Monte Carlo simulation. We note that the agreement deteriorates for $\sqrt{x_L}Q \lesssim 10$ GeV, due to the fact that the EEC suffers from soft-gluon effects at the level of sub-leading power corrections. Nevertheless, it can be also seen that soft gluon effects are suppressed for the ratio compared to EEC itself, as reflected in Fig. 7. It would be interesting to quantify how the quantum scaling affects extractions of the strong coupling constant from the E3C/EEC ratio, which we leave for future work.